ELSEVIER

Journal of Alloys and Compounds 455 (2008) 497–500

Journal of ALLOYS AND COMPOUNDS

www.elsevier.com/locate/jallcom

Structural and photoluminescence properties of europium-doped titania nanofibers prepared by electrospinning method

Jianguo Zhao, Changwen Jia, Huigao Duan, Zhiwen Sun, Xiaoming Wang, Erqing Xie *,[1]

School of Physical Science and Technology, Lanzhou University, Lanzhou 730000, China

Received 14 December 2006; received in revised form 26 January 2007; accepted 30 January 2007
Available online 3 February 2007

Abstract

In this letter, we have studied photoluminescence (PL) properties of europium-doped titania (TiO_2:Eu^{3+}) nanofibers fabricated by electrospinning. The nanostructured TiO_2:Eu^{3+} is characterized by field emission scanning electron microscopy (FESEM), X-ray diffraction (XRD), Raman spectrum. When TiO_2:Eu^{3+} nanofibers are excited by 325 nm, their emission spectrum show emission lines associated with intra-4f transitions from $^5D_1$ and $^5D_0$ levels to ^7F_j level of Eu^{3+} ions. In addition, the concentration quench effect, energy transfer and photoluminescence mechanism in TiO_2:Eu^{3+} nanofibers are also discussed.

Keywords: Europium-doped titania; Electrospinning; Nanofiber; Energy transfer; Photoluminescence

1. Introduction

In recent years, dimensionally modulated materials with integrated platform of nanostructured metallic or semiconducting materials are highly desirable for advanced nanoscale electronic and optoelectronic applications [1–4]. Rare earth compounds have been widely used as high-performance luminescent devices, magnets, catalysts, and other functional materials [5,6]. It has been reported that the luminescent quantum efficiency of Eu^{3+} in nanowires was enhanced more considerably than that of the corresponding nanoparticles and the bulk powders [7]. Some wide band-gap semiconductors including Y_2O_3 [8], AlN [9], GaN [10], ZnO [11], TiO_2 [12] have been selected as host materials in order to excite rare earth ions efficiently and to yield intense luminescence. Among these materials, TiO_2 is attractive as a promising semiconductor with outstanding optical and thermal properties. It is a good candidate to be used as the host material of rare earth. TiO_2:Eu^{3+} nanopowder and thin films have been widely studied [13,14]. But its nanofibers fabricated by electrospinning have not been investigated yet.

Electrospinning technique has been found to be unique and cost-effective approach for manufacturing large surface area membranes for a variety of applications [15,16]. The first patent that described the operation of electrospinning appeared in 1934 [17]. Electrospinning is a process by which high static voltages are used to produce nano- and microscale fibers, with the fiber diameter in the range from less than 10 nm to over several micrometers. This technique can be used with a variety of polymers to produce nanoscale fibrous membranes. Electrospun nanofibres may have surface area to volume ratio approximately one to two orders of magnitude more than that of in continuous thin films [18].

In this work, we demonstrate, for the first time to our knowledge, the structural and luminescent properties of TiO_2:Eu^{3+} nanofibers through the method of electrospinning. The structural of samples annealed at different temperatures were investigated. PL measurements were performed for different ratio Eu^{3+}-doped TiO_2 with above band excitation. The mechanism of PL was discussed.

2. Experimental

2.1. Sample preparation

TiO_2:Eu^{3+} nanofibers were prepared by electrospinning. In the first step, 0.5 g of tetra-*n*-butyl titanate ($Ti(OC_4H_9)_4$) europium nitrate (1, 2, 3 and

* Corresponding author.
E-mail addresses: zhaojiang04@lzu.cn (J. Zhao), xieeq@lzu.edu.cn (E. Xie).
[1] Tel.: +86 931 891 2703; fax: +86 931 891 3554.

0925-8388/$ – see front matter © 2007 Published by Elsevier B.V.
doi:10.1016/j.jallcom.2007.01.153

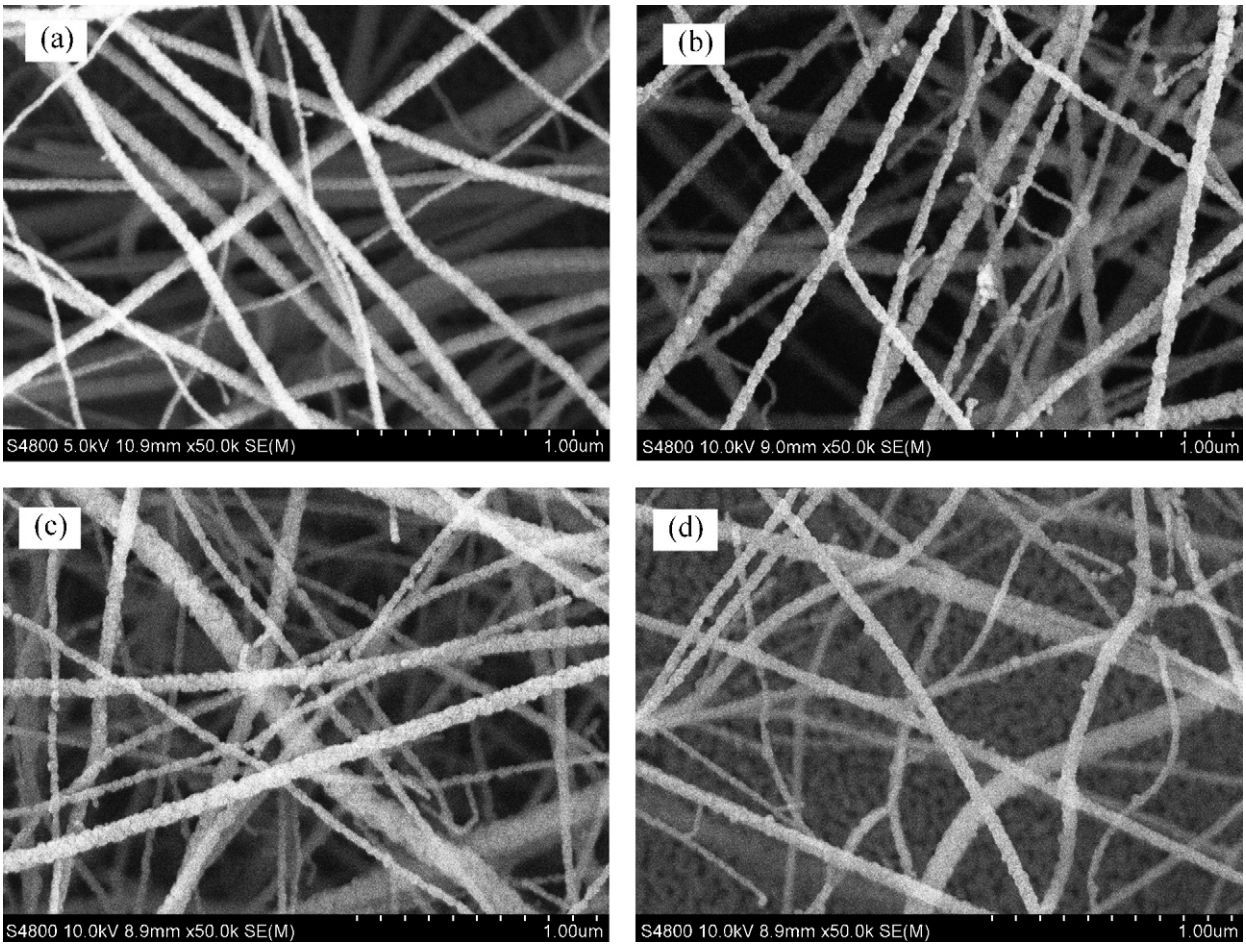

Fig. 1. SEM images of TiO_2:Eu^{3+} (the Eu^{3+} concentration, i.e. molar ratio in the samples): (a) 1%; (b) 2%; (c) 3%; (d) 10%.

10 mol%) was mixed with 1 ml of ethanol and 1 ml of acetic acid as a catalyst in a measuring cylinder. After 20 min, this solution was added to 2 ml of ethanol that contained 0.2 g polyvinylpyrolidone (PVP) (Sigma–Aldrich, $M_w \approx 1{,}300{,}000$) and 0.5 ml of *N*,*N*-dimethyl formamide (DMF), followed by magnetic stirring for ~1 h. The electrospinning solution was taken in a syringe equipped with a stainless needle. The needle was connected to a high-voltage power supply that is capable of generating dc voltages up to 60 kV. A plate of aluminium foil as the collection screen was placed at a distance of 15 cm from the needle tip and silicon wafers were held on the screen to be used as substrates. Then the electric voltage of 25 kV was applied between the stainless needle and the collector. The electrospinning process was finished in air and the deposition was conducted for 20 min so that dense mats were obtained. The as-spun composite nanofibers on silicon wafers were left in air for ~24 h to make $Ti(OC_4H_9)_4$ hydrolyze completely. In order to increase the crystallinity of the materials and reduce the presence of OH and organic groups, which are responsible for the luminescence quenching, the TiO_2:Eu^{3+} nanofibers were annealed under air atmosphere for 3 h at 873 K because at this temperature the samples have good crystallinity and pure anatase phase.

2.2. Characterization of nanofibers

FESEM images of the sample were recorded by Hitachi S-4800 scanning electron microscope. The crystal structure of TiO_2:Eu^{3+} nanofibers were characterized by X-ray diffractometer (Philips, X'pert Pro) with a monochromatized source of Cu Kα radiation at a wavelength of 0.15405 nm. Raman spectra of nanofibers were measured at room temperature using the 532 nm of an Ar+ laser as an exciting source (JY-HR800). Room temperature PL emission spectra of TiO_2:Eu^{3+} nanofibers were recorded using a 325 nm He–Cd laser as an excitation source.

3. Results and discussion

FESEM images of the TiO_2:Eu^{3+} nanofibers after annealing at 873 K are shown in Fig. 1 for different concentrations. The nanofibers are randomly oriented on the substrate because of the bending instability associated with the spinning jet. The diameter of composite nanofibers is between 20 and 100 nm, and the length can even reach to decimeter grade. There is no obvious change for nanofibers diameter with increase in europium content. It can also be seen that the surfaces of the nanofibers show different shrinkage and roughness with different europium content.

The XRD patterns of obtained TiO_2:Eu^{3+} nanofibers annealed in air at 873 K are present in Fig. 2. The samples showed a series of broad peaks at $2\theta = 25.2$, 38, 44.6, 48 and 55.1, corresponding to those of pure anatase TiO_2 (JCPDS 21-1272). Eu^{3+} ions are hardly substituted with Ti^{4+} ions due to the large difference on the ionic radius between Ti^{4+} and Eu^{3+}. (The ionic radii of Ti^{4+} and Eu^{3+} are 0.745 and 1.087 Å, respectively.) So the Eu–O–Ti bonds are only formed on the crystalline surface or interstitials of TiO_2 nanoparticles. At Eu^{3+} concentration of 3%, the Eu–O–Ti bonds may be saturated. With the Eu^{3+} ions concentration increasing, no additional phase was found and diffraction peaks related to Eu^{3+} compound could not be detected. We can explain why the redundant Eu^{3+} ions do

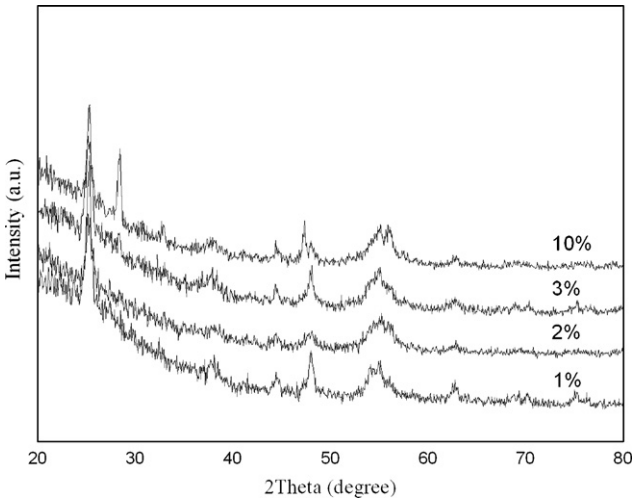

Fig. 2. XRD patterns of TiO_2:Eu^{3+} nanofibers (the Eu^{3+} concentration, i.e. molar ratio in the samples, is 1, 2, 3 and 10%).

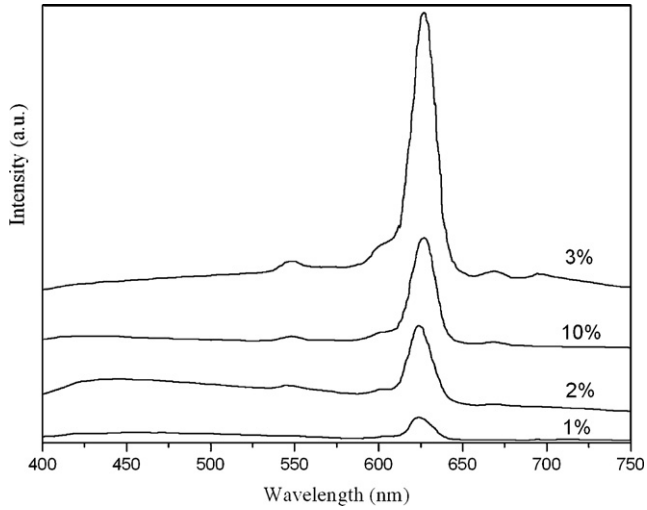

Fig. 4. PL spectra of TiO_2:Eu^{3+} nanofibers (Eu^{3+} concentration is 1, 2, 3 and 10%) at room temperature, excited by 325 nm.

not appear in XRD spectrum using core–shell structure. The nanocomposites with the structure of TiO_2 shell and Eu_2O_3 nanometer size cores were considered to be produced through the hydrolysis and condensation process. It is shown that there is no change of global structure for samples doped with different concentration of Eu^{3+} ions annealed at 873 K.

The Raman spectra of TiO_2:Eu^{3+} nanofibers with different concentration are shown in Fig. 3. Besides the spectrum from Si (1 0 0) substrate is dominated by the zone-center optical phonon O (Γ) peak of bulk Si at 520 cm^{-1} [19], anatase peaks at 147, 400 and 638 cm^{-1} can also be seen clearly (space group $I4_1/amd$), which are agreement with the literature report [20]. 639, 197 and 147 cm^{-1} are assigned to the E_g modes and the band at 400 cm^{-1} to the B_{1g} mode of the TiO_2 anatase phase. These peak frequencies in the Raman spectra of these nanofibers match those of single anatase crystal at room temperature. From this figure we can see that the doping of Eu^{3+} does not change the structure of TiO_2. This is consistent with the XRD patterns.

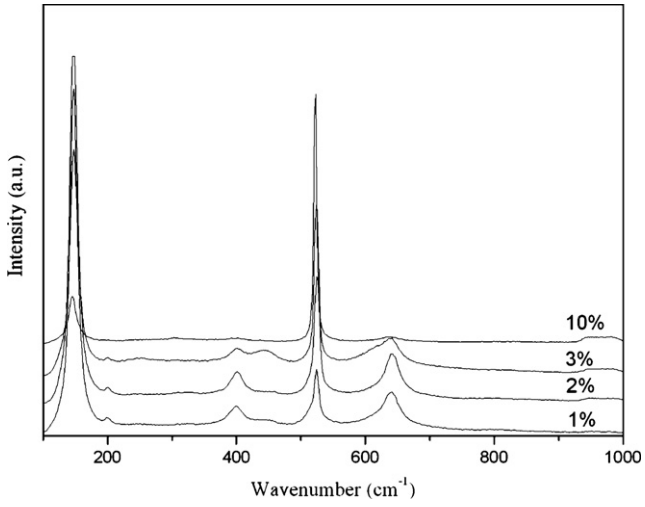

Fig. 3. Raman spectra of TiO_2:Eu^{3+} nanofibers for Eu^{3+} concentrations of 1, 2, 3 and 10%.

Fig. 4 shows the emission spectra of different doping Eu^{3+} ions in TiO_2 host (1, 2, 3 and 10 mol%). The nanofibers are excited with above band-gap energy (325 nm). In general, characteristic Eu^{3+} PL emission involves transitions from the excited $^5D_0$, $^5D_1$ level to the crystal-field-split ^7F_j manifolds of the $4f^6$ electronic configuration. The peaks at 600, 621, 667 and 695 nm are assigned to the intra-4f transitions of $^5D_0 \rightarrow {}^7F_j$ ($j = 1$–4) of Eu^{3+} ions. The 545 nm emission can be ascribed to the $^5D_1 \rightarrow {}^7F_1$ transition. From Fig. 4, it can be seen that the $^5D_0$ emission of Eu^{3+} is intensified with the increase in Eu^{3+} content, and the emission intensity is the strongest at about 3% of Eu^{3+} concentration. But at higher Eu^{3+} concentration, the emission intensity of Eu^{3+} is decreased. This is the concentration quench effect, which can be explained by the cross-relaxation [21]. At Eu^{3+} concentration of 3%, the Eu–O–Ti bonds may be saturated, and at higher concentration the spatial separation between Eu^{3+} ions becomes smaller and cross-relaxation rate is higher. Therefore, the fluorescence intensity is decrease at higher Eu^{3+} concentrations. It can be seen there are only Eu^{3+} emissions without the background of the broad emission of TiO_2. In pure anatase TiO_2 thin films, a broad photoluminescence is observed at about 550 nm [12]. This is attributed to the radiative recombination of self-trapped excitons.

We also fabricated pure TiO_2 thin films. A broad photoluminescence at about 550 nm is attributed to the radiative recombination of self-trapped excitons. After doping Eu^{3+} in TiO_2 host, we cannot find this broad peak. We use Fig. 5 to explain it: the excitation of 325 nm laser leads to the transition of electron in TiO_2 matrix from valance to conduction band. Some of the excited electrons in conduction band transit non-radiatively to $^5D_0$ and $^5D_1$ levels of Eu^{3+} ions, other excited electrons are captured by trap, forming self-trapped excitons. This is the original of the broad emission band that is found in pure TiO_2 nanofibers. Here, E_g is the band-gap of the TiO_2 and ΔE is the depth of the carrier trap level. To excite the Eu^{3+} 4f shell by self-trapped excitons, the $E_g - \Delta E$ has to be larger than or equal to Eu 4f, which is the energy needed to excite the Eu

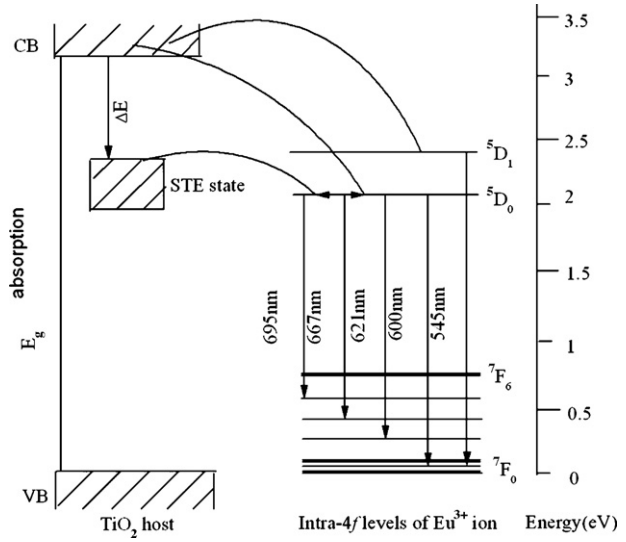

Fig. 5. Excitation and emission mechanisms for TiO_2:Eu^{3+} nanofibers.

4f shell. Using this we can say that the energy transfer occurs between self-trapped excitons and Eu^{3+} 4f shell after we doped Eu^{3+} in TiO_2 nanofibers.

4. Conclusion

TiO_2:Eu^{3+} nanofibers with different concentration are prepared by electrospinning. With the increase of concentration of Eu^{3+} in TiO_2 host, PL intensity in visible range due to Eu^{3+} ions increases at first but then decreases, and reaches maximum when the concentration of Eu^{3+} ions is 3%. This is the concentration quench effect. Comparing with pure TiO_2 nanofibers, energy transfer from STE state to Eu^{3+} is considered to be the reason why the peak at 550 nm disappears after doping in TiO_2 nanofibers.

References

[1] B.S. Simpkins, P.E. Pehrsson, A.R. Laracuente, Appl. Phys. Lett. 88 (2006) 072111.
[2] A.V. Murugan, A.K. Viswanath, B.A. Kakade, V. Ravi, V. Saaminathan, J. Phys. D 39 (2006) 3974.
[3] M. Kanoun, C. Busseret, A. Poncet, A. Souifi, T. Baron, E. Gautier, Solid-State Electr. 50 (2006) 1310.
[4] L. Li, Y.W. Yang, X.H. Huang, G.H. Li, R. Ang, L.D. Zhang, Appl. Phys. Lett. 88 (2006) 103119.
[5] H.Q. Chiang, J.F. Wager, R.L. Hoffman, J. Jeong, D.A. Keszler, Appl. Phys. Lett. 86 (2005) 013503.
[6] W. Park, J.S. Kim, G.C. Yi, M.H. Bae, H.J. Lee, Appl. Phys. Lett. 85 (2004) 5052.
[7] H. Song, L. Yu, S. Lu, T. Wang, Z. Liu, L. Yang, Appl. Phys. Lett. 85 (2004) 840.
[8] J. Zhang, G. Hong, J. Solid State Chem. 177 (2004) 1292.
[9] F.S. Liu, H.W. Dong, Q.L. Liu, J.K. Liang, J. Luo, Y. Zhang, L.T. Yang, G.H. Rao, Opt. Mater. 28 (2006) 1029.
[10] R. Kudrawiec, M. Nyk, A. Podhorodecki, J. Misiewicz, W. Strek, M. Wolcyrz, Appl. Phys. Lett. 88 (2006) 061916.
[11] A. Ishizumi, Y. Kanemitsu, Appl. Phys. Lett. 86 (2005) 253106.
[12] C.W. Jia, E.Q. Xie, J.G. Zhao, Z.W. Sun, A.H. Peng, J. Appl. Phys. 100 (2006) 023529.
[13] A.C. Gallardo, M.G. Rocha, I.H. Calderon, R.P. Merino, Appl. Phys. Lett. 78 (2001) 3436.
[14] B. Julian, R. Corberan, E. Cordoncillo, P. Escribano, B. Viana, C. Sanchez, Nanotechnology 16 (2005) 2707.
[15] C.M. Vaz, S.V. Tuijl, C.V.C. Bouten, F.P.T. Baaijens, Acta Biomater. 1 (2005) 575.
[16] Z.W. Ma, M. Kotaki, S. Ramakrishna, J. Membr. Sci. 265 (2005) 115.
[17] A. Formalas, US Patent 1975, 504 (1934).
[18] P. Gibson, H.S. Gibson, D. Rivin, Coll. Surf. A 469 (2001) 187.
[19] S.K. Mohanta, R.K. Soni, S. Tripathy, C.B. Soh, S.J. Chua, D. Kanjilal, Physica E 35 (2006) 42.
[20] B. Karunagaan, K. Kim, D. Mangalaraj, J. Yi, s. Velumani, Sol. Energ. Mater. Sol. C 88 (2005) 199.
[21] R. Schmechel, M. Kenndy, H.V. Seggern, H. Winkler, M. Kolbe, R.A. Fischer, X. Li, A. Benker, M. Winterer, H. Hahn, J. Appl. Phys. 89 (2001) 1679.